Effect of Normal Breathing and Breath Holding on Seismocardiographic Signals and Heart Rate

Tanvir Hassan, Badrun Rahman, Richard H. Sandler, Hansen A. Mansy

Biomedical Acoustic Research Lab, University of Central Florida, Orlando, Florida, USA

Biomedical Acoustic Research Company, Orlando, Florida, USA

Outline

- Introduction
  - Motivation
  - Background
  - SCG Variability through Respiration
- Objectives and Expected Outcome
- Methods
  - Data Acquisition
  - Experimental Protocol
  - Filtering, Segmentation and Clustering
- Results
  - Cluster Distribution
  - Feature Analysis
- Conclusions and Future Work

Introduction - Motivation

- Heart disease is a leading global cause of mortality [1].
- On average someone dies of cardiovascular disease (CVD) every **36 seconds** in the US [1] .
- The average annual direct and indirect cost of CVD in the US was estimated to be **$363.4 billion dollars** from 2016 to 2017 [1].
- By 2035, approximately **130 million adults** in the US population (45.1%) are projected to have developed some form of cardiovascular disease [1].
- An earlier study predicted that heart failure will increase approximately **46%** from 2012 to 2030 in adults [1].
- The estimated total cost of CVD is expected to reach **$1.1 trillion dollars** by 2035 [1].

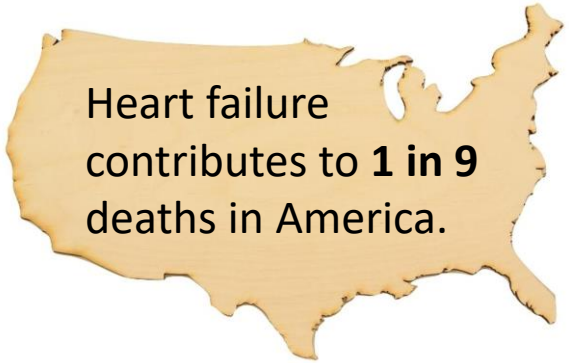

[1] Salim S. Virani et al., “Heart disease and stroke statistics—2021 update: a report from the American Heart Association,” Circulation, vol. 143, pp. e254–e743, 2021.

Introduction - Background

- Seismocardiographic signals (SCG) are vibrations induced by the heart activity measured non-invasively at the chest surface .
- These vibrations are correlated to the mechanical processes surrounding the heart such as valve closure, blood momentum changes and cardiac muscle contraction.
- SCG signals can draw out valuable information about heart function and can be potentially utilized to diagnose cardiac diseases.
- SCG was described as early as 1961 [2].
- Other studies extracted different cardiac parameters, such as heart rate or systolic time intervals monitoring, from SCG signals [3-4].
- Despite its high utility, little information is available regarding signal variability during different breathing maneuvers.
- To increase SCG utility for monitoring HF patients, it is important to have adequate knowledge about the morphological variation of the SCG signal.

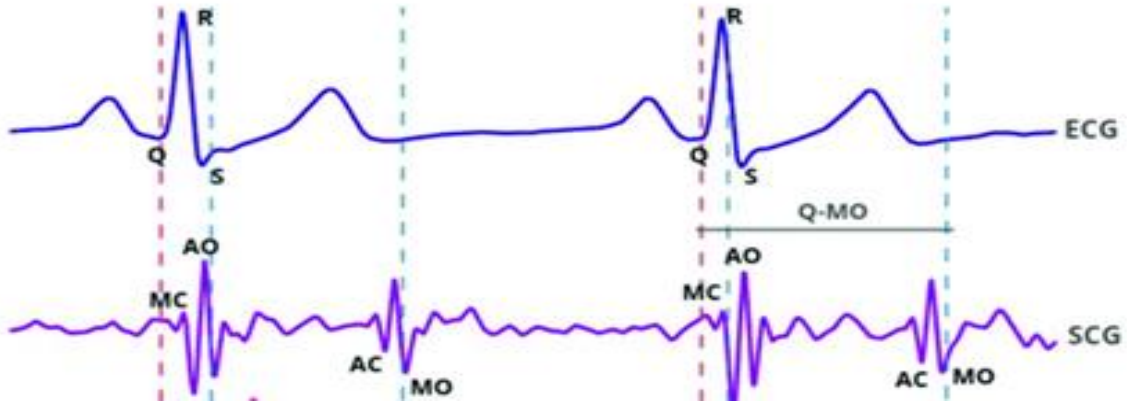

The cardiac events identified in the SCG signal as proposed by Crow et al (1994). The abbreviations are:

MC: *mitral valve closure*, **AO**-*aortic valve opening*,

AC- *aortic valve closure*, **MO**-*mitral valve opening*

[2] B. S. Bozhenko, "Seismocardiography--a new method in the study of functional conditions of the heart," Ter. Arkh., vol. 33, p. 55, 1961.
[3] D. M. Salerno, "Seismocardiography: A new technique for recording cardiac vibrations. concept, method, and initial observations," J. Cardiovasc. Technol., vol. 9, no. 2, pp. 111–118, 1990.
[4] K. Tavakolian et al., "Myocardial contractility: A seismocardiography approach," in Engineering in Medicine and Biology Society (EMBC), 2012 Annual International Conference of the IEEE, 2012.

Introduction: SCG Variability through Respiration

- SCG has a potentially high clinical utility which is limited by signal variability.
- SCG utility can be improved by decreasing its variability and enhanced understanding of variability sources.
- One known source of variability is breathing.
- During breathing there are changes in the heart position (due to the movement of the heart, diaphragm and lungs), intrathoracic pressure (i.e., pressure around the heart) and heart rate.
- These changes may introduce errors in SCG interpretation yet may contain important SCG morphological features diagnostic value.
- To our knowledge, there is limited published information about SCG changes during respiratory maneuvers (such as breath holding).

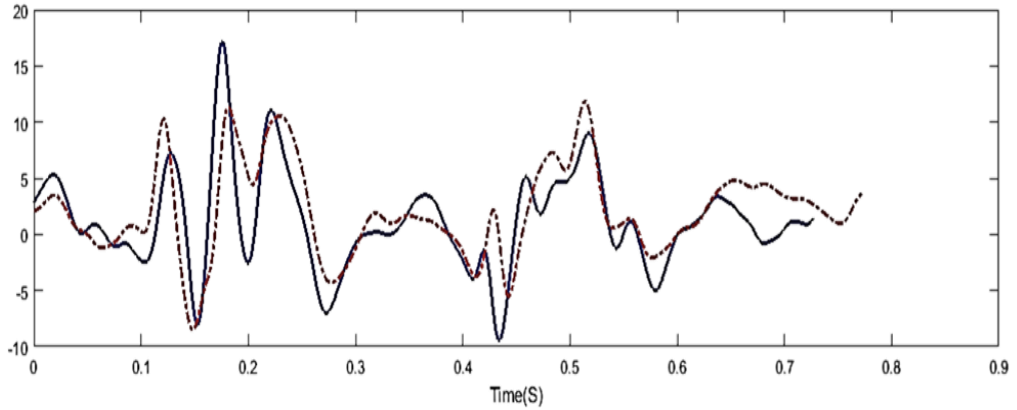

Objectives and Expected Outcome

Objectives:

- Reduce SCG signal variability during normal breathing by clustering using unsupervised machine learning.
- Compare the following SCG and heart rate features between normal breathing and breath holding (at end inspiration and end expiration).
  i. Intra cluster variability
  ii. Normalized SCG energy in 0-20 Hz
  iii. Heart rate
  iv. Heart rate variability in the “high frequency” range 0.15-0.4 Hz

Outcome: Documentation of SCG and HR changes under different breathing states.
I) Enhance our understanding of SCG sources; II) Suggest optimum breathing states for recording SCG.

Methods

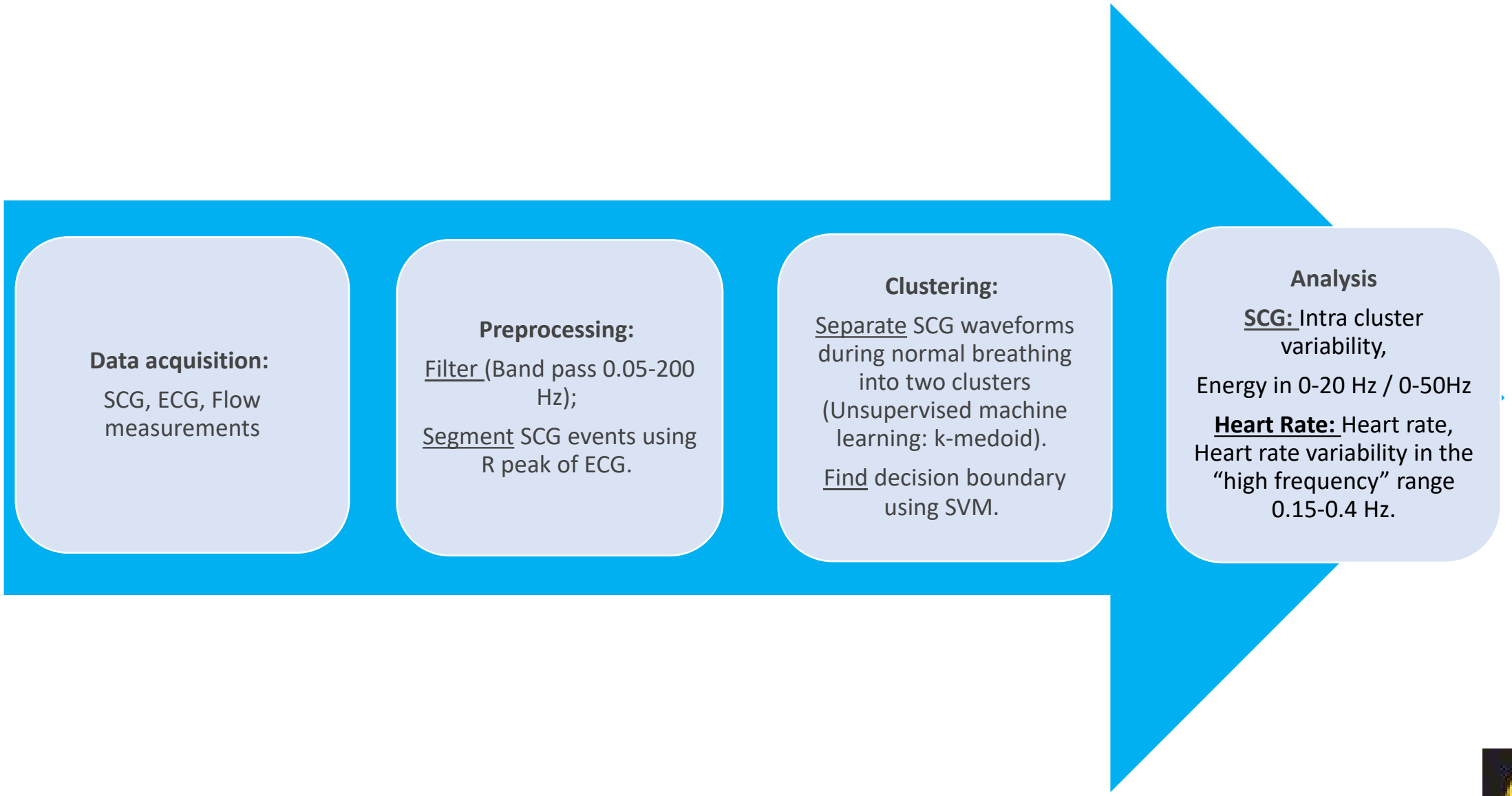
Data acquisition:
SCG, ECG, Flow measurements
Preprocessing:
Filter (Band pass 0.05-200 Hz);
Segment SCG events using R peak of ECG.
Clustering:
Separate SCG waveforms during normal breathing into two clusters (Unsupervised machine learning: k-medoid).
Find decision boundary using SVM.
Analysis
SCG: Intra cluster variability,
Energy in 0-20 Hz / 0-50Hz
Heart Rate: Heart rate, Heart rate variability in the "high frequency" range 0.15-0.4 Hz.

Methods: Data Acquisition

- SCG sensor : Tri-axial Accelerometer (PCB Piezotronics); Sensitivity: 100 mV/g
- SCG signal amplifier: Model 480B21, (PCB Piezotronics)
- Respiration sensor: Spirometer (SP-304, iWorx Systems)
- ECG sensor: IX-B3G biopotential recorder (iWorx Systems)
- Data acquisition: IX-RA-834 (iWorx Systems)

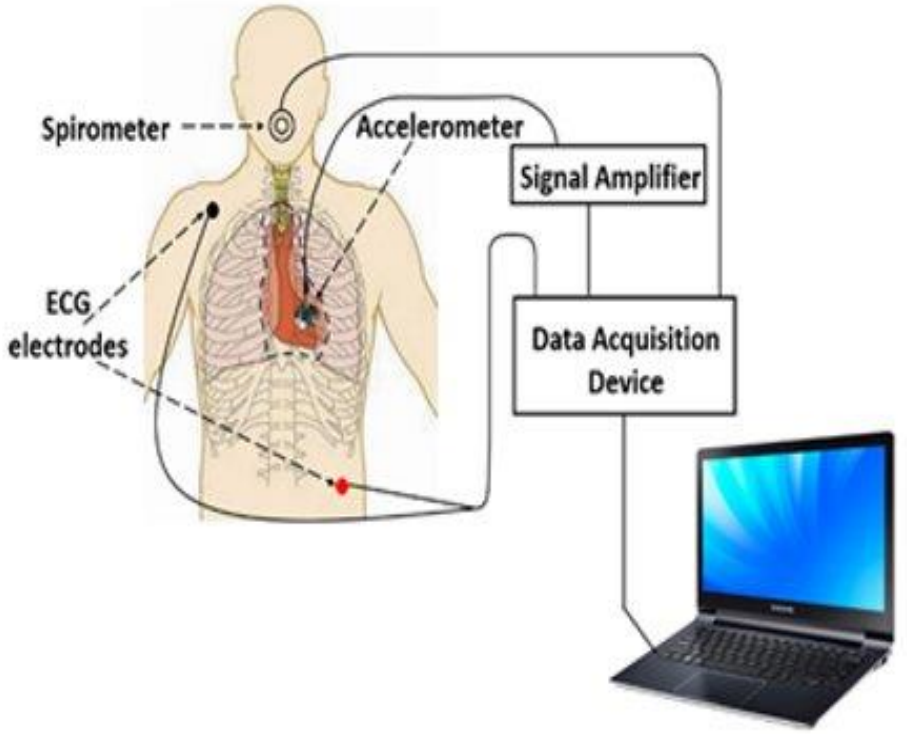

- SCG, electrocardiography (ECG) and airflow signals were simultaneously acquired .
- Sampling Frequency: 10 kHz

Methods: Experimental Protocol

- All studies done with a face mask covering the nose and mouth connected to the spirometer.

Normal Breathing:

- Subjects rest for 2 mins while breathing through spirometer. Baseline tidal volume is measured.
- Subjects practice breathing at tidal volume within +/-10-20% of their baseline.
- Subjects continue to maintain a tidal volume +/-10-20 % of their baseline for 5 mins while recording tri-axial SCG, ECG, spirometer flow rate.

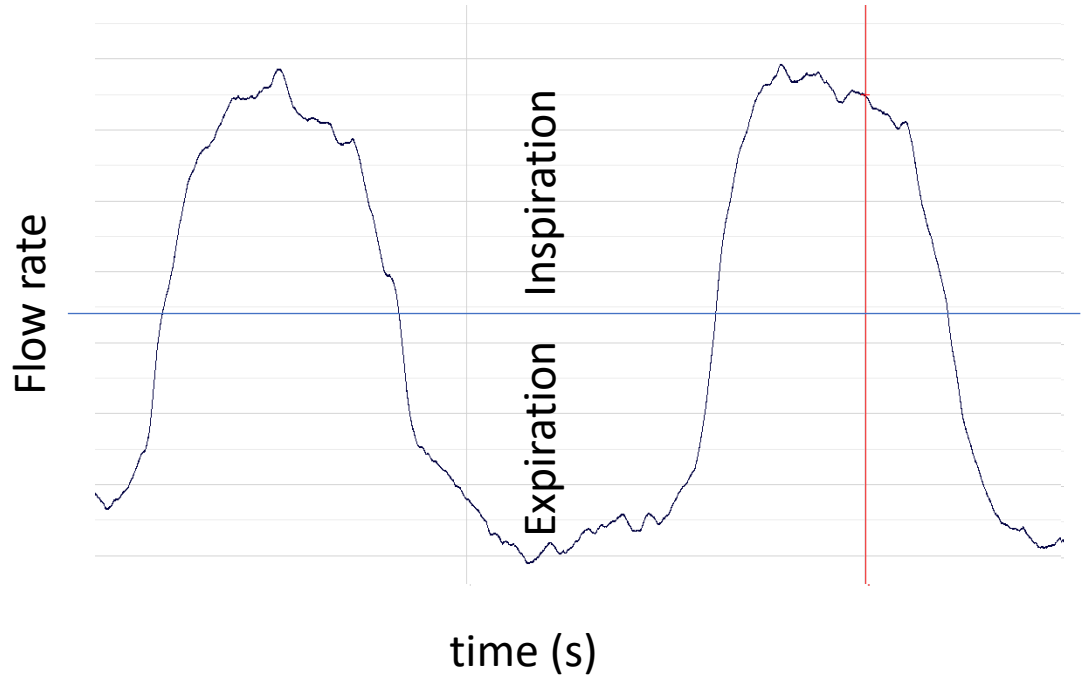

Methods: Experimental Protocol

Breath hold (while maintaining an open glottis):

- ❑ End inspiration breath hold for 20s while recording the signals.
- ❑ Rest for 3 min.
- ❑ Repeat the record–and-rest cycle 2 more times (total of 3 cycles for end inspiration).
- ❑ End expiration breath hold for 20s while recording the signals.
- ❑ Rest for 3 min.
- ❑ Repeat the cycle 2 more times (total of 3 cycles for end expiration).

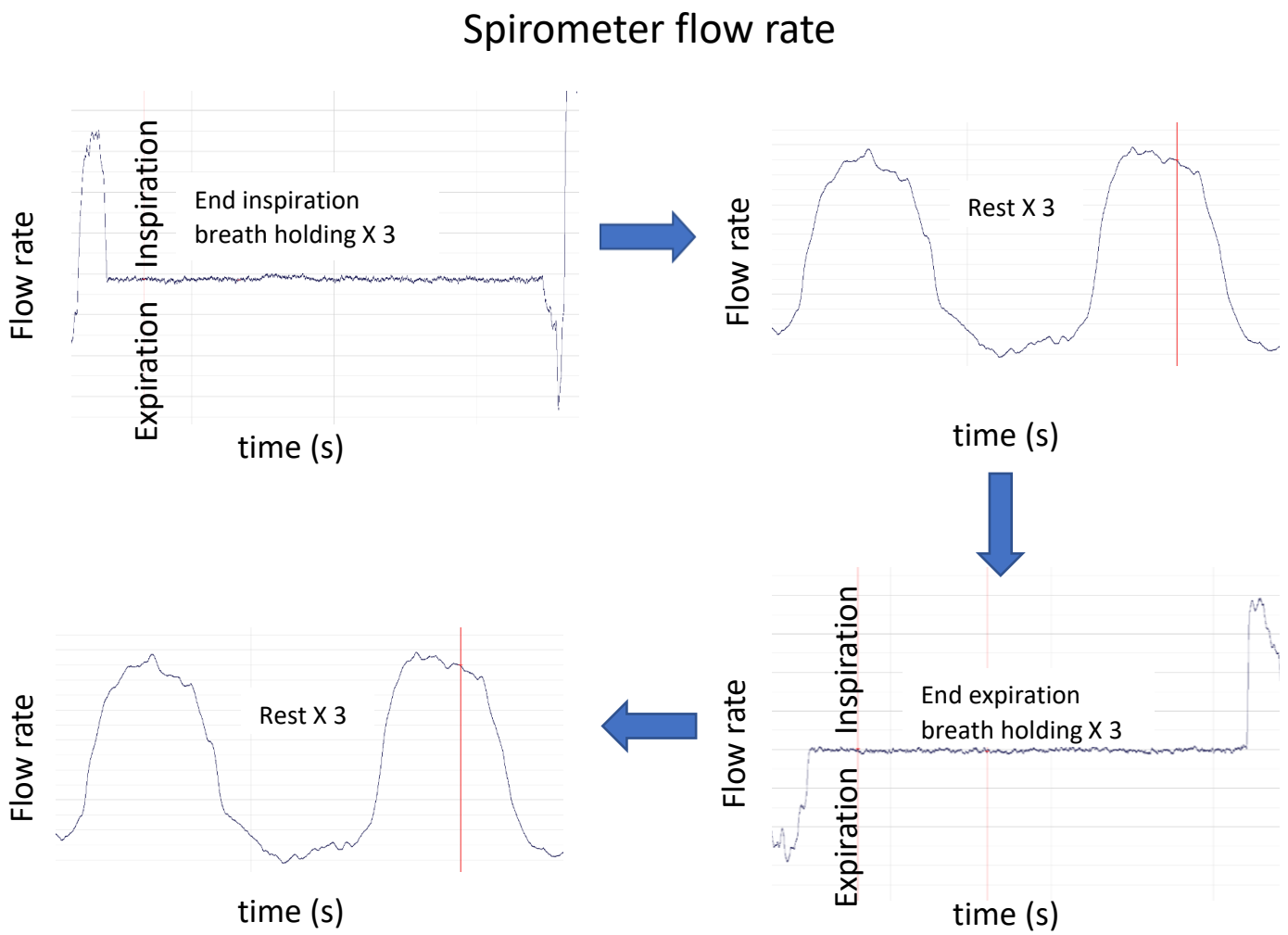

Methods: Filtering, Segmentation and Clustering

- Filtering: 4th order Chebyshev 2 type band-pass filter with a cut off 0.05-200 Hz after down sampling the signals to 1000 Hz. This is done to reduce background noise and baseline wandering due to respiration.

- Segmentation: Pan Tompkins algorithm was used to detect R peaks of ECG events. Each SCG event was selected to start 0.1 seconds before the R peak of the corresponding ECG and ends at 0.1 seconds before the next R peak.

- Clustering: An unsupervised machine learning technique (k-medoid clustering) was used to cluster SCG events based on their morphology to reduce SCG variability during normal breathing. Here, dynamic time warping (DTW) distance was used to perform the clustering.

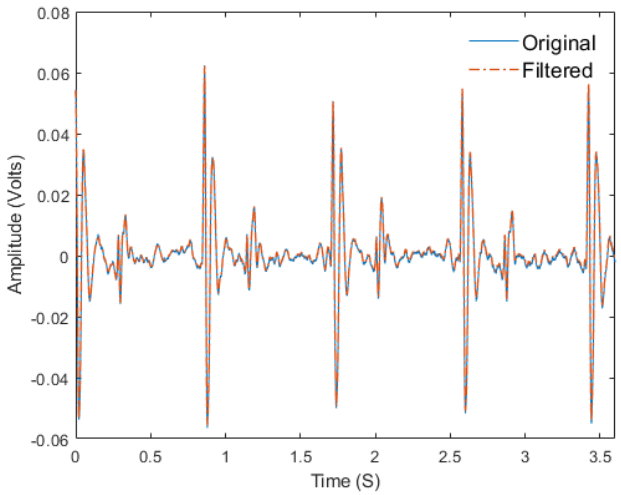

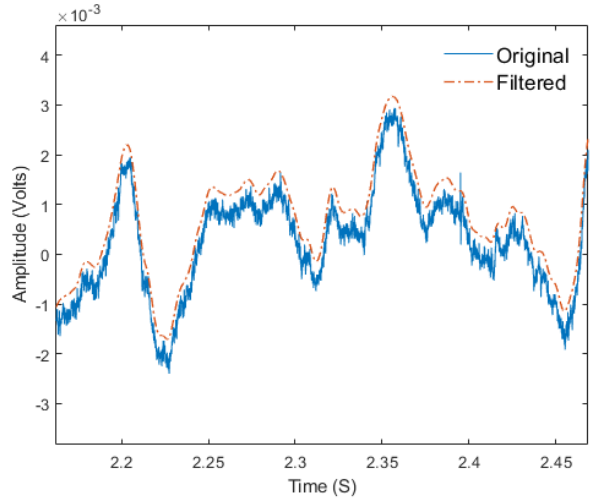

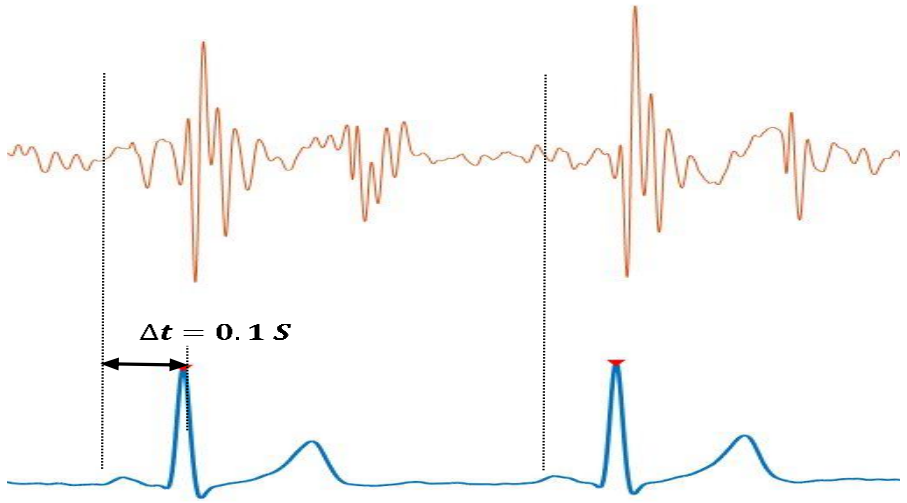

Methods: Dynamic Time Warping (DTW)

- Optimal global alignment between two time sequences, exploiting temporal distortions between them.
- Measure similarity between two sequences which may vary in time.

$$D(i,j) = \delta(x_i, y_j) + min \begin{cases} D(i, j-1) \\ D(i-1, j) \\ D(i-1, j-1) \end{cases}$$

where $\delta(x_i, y_j) = (x_i - y_j)^2$ *or* $|x_i - y_j|$

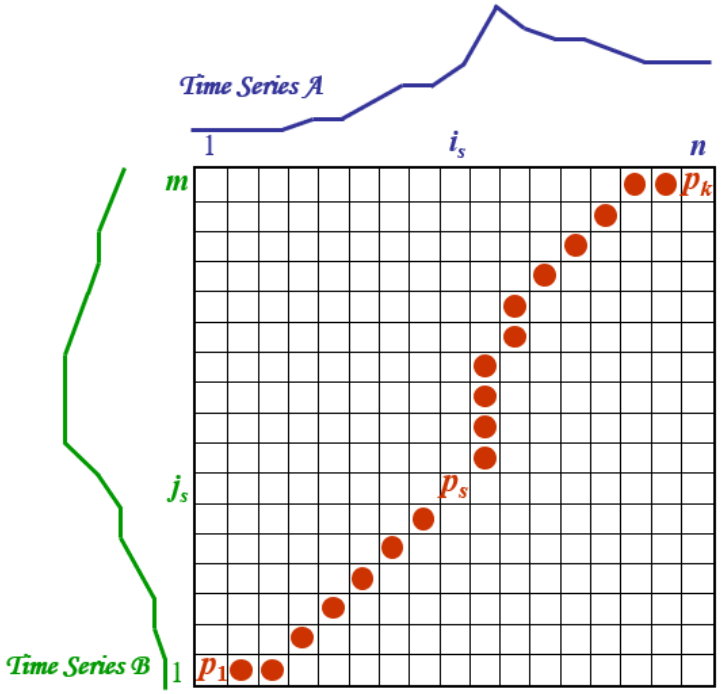

DTW finds the *best alignment* between $\mathcal{A}$ and $\mathcal{B}$ by finding the path through the distance matrix

$$P = p_1, \ldots, p_s, \ldots, p_k$$

$$p_s = (i_s, j_s)$$

which *minimizes* the total distance between them.

Methods: K-medoid Clustering

- Inputs: Number of clusters= K. Set of SCG beats: $S = \{X_1, X_2, X_3, \dots, X_i \dots, X_N\}$ where each beat is defined by its feature vector (amplitude) as $X_i = \{x_1, x_2, x_3, \dots, x_{l_i}\}$
- Step 1: Initialize $C_1, \dots, C_j, \dots C_k$ as the **medoids** for each cluster
- Step 2: For each X_i find the nearest C_j using DTW as the distance measure and assign X_i to cluster j
- Step 3: Update medoids, C_j, based on the clustered events from step 2 using Equation,

$$C_j = argmin_{y \in \{X_{1j}, X_{2j}, \dots, X_{ij}, \dots, X_{nj}\}} \sum_{i=1}^{n_j} dtw(y, X_{ij})$$

  where, X_{ij} is the i^{th} sequence belongs to cluster j and n_j is the number of sequences belong to C_j after step 2.

- Step 4: Repeat step 2 and 3 till none of the cluster assignments change.

Methods: Optimum Clusters

- The elbow method was applied to find the optimum number of clusters.
- The method determines the minimum cluster number by optimizing intra-cluster variability.
- The intra-cluster variability was measured by the average sum of distances (SOD).

$$SOD = \frac{1}{N}\sum_{j=1}^{k}\sum_{i=1}^{n_j} dtw(C_j, X_{ij})$$

X_{ij} : ***i*** th events belonging to cluster medoid C_j

n_j : The number of events belong to C_j .

N: Total number of events used in the clustering.

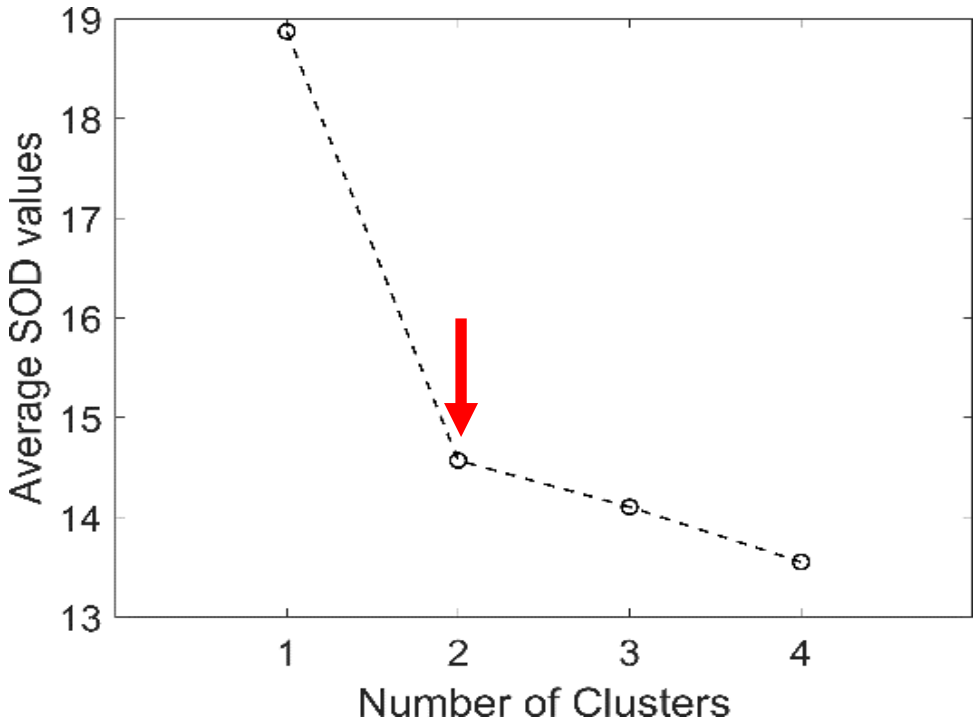

Methods: Decision Boundary using Support Vector Machine

- SVM algorithm finds a hyperplane for n number of features such that the margin between the classes is maximized.
- For a linearly separable data, a decision boundary can be defined as $w.x_i + b = 0$ where the margins are defined using the hyperplanes $w.x_i + b = \pm 1$.
- The support vectors are defined as the marginal data points on the boundary.
- Here w, x, and b are the weight vector, feature vector, and the bias, respectively.
- SVM focusses on maximizing the decision margin $d = \frac{1}{\|w\|}$.

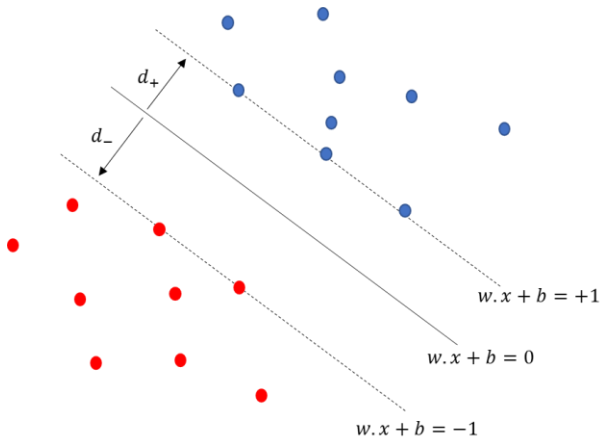

Accuracy= (TP+TN)/(TP+FP+FN+TN)

Results: Cluster Distribution

Accuracy: 0.9750

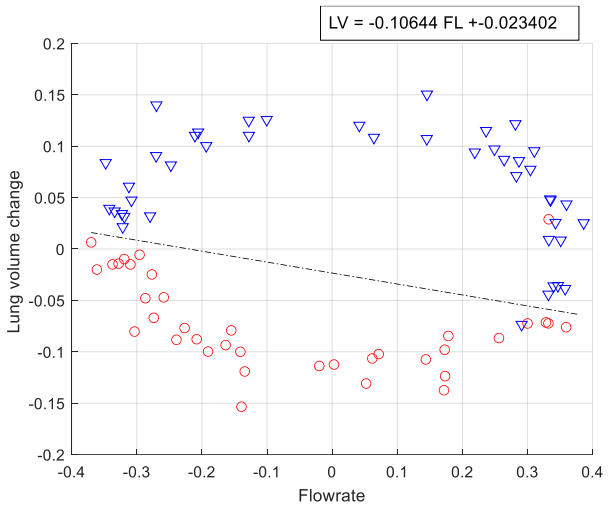

Accuracy: 0.9851

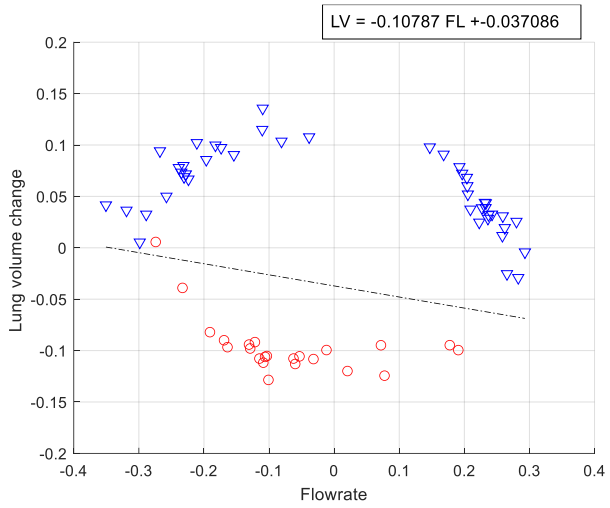

- The SCG clustering correlates with respiration, and the two clusters were well separated with high accuracy (>80% in all subjects).
- SCG events belonging to cluster 1 and cluster 2 are labeled as blue '∇' triangles and red 'o' circles, respectively.
- <u>Findings:</u> clusters are not completely separated based on respiratory flow rate (i.e., inspiration vs expiration phase) or by lung volume (i.e., high lung volume vs low lung volume).

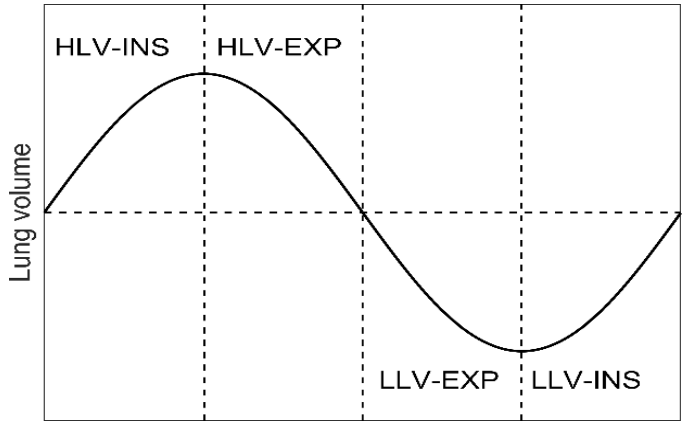

The four respiratory phases labeled in a simplified lung volume waveform Here,

INSP- Inspiratory phase.
EXP – Expiratory phase.
HLV - High lung volume phase
LLV - Low lung volume phase.

- This clustering pattern was consistent for all study subjects.

Results: Feature Analysis

- The SCG variability (intra cluster) was calculated using the Dynamic Time Warping (DTW) distance of SCG waveforms in the time domain.

  Equation used to calculate the intra cluster DTW distances:

$$\boldsymbol{Intra - cluster\ DTW} = \frac{\mathbf{1}}{\boldsymbol{n1+n2}} \left[\sum_{\boldsymbol{i=1}}^{\boldsymbol{n_1}} \boldsymbol{dtw}(\boldsymbol{C_1}, \boldsymbol{X_{i1}}) + \sum_{\boldsymbol{i=1}}^{\boldsymbol{n_2}} \boldsymbol{dtw}(\boldsymbol{C_2}, \boldsymbol{X_{i2}})\right]$$

  Here, X_{i1}, X_{i2} are the ith SCG event belonging to cluster 1 and cluster 2, respectively while C_1 and C_2 are the respective cluster medoids. And n_1, n_2 are the total number of events belong to cluster 1 and 2, respectively. Well separated clusters are expected to have relatively low intra-cluster DTW distance.

- The energy of the SCG within 0-20 Hz normalized by the energy in the 0-50 Hz (has utility [5]).
- Heat rate spectral power was calculated in 0.15–0.4 Hz (known as high frequency range (HF).

[5] P. Gamage, "Seismocardiography - Genesis, and Utilization of Machine Learning for Variability Reduction Improved Cardiac Health Monitoring," Department of Mechanical and Aerospace Engineering, University of Central Florida, Orlando, FL, 2020.

Results: Feature Analysis

Intra-cluster variability (p<0.05)

Change in intra-cluster variability	Mean (%)	SD(%)
(After clustering -before clustering)/ before clustering	**-20**	**9**
(End inspiration- Normal breathing)/Normal breathing	**-29**	**20**
(End Expiration- Normal breathing)/Normal breathing	**-35**	**19**

Heart rate (p<0.05)

Change in HR during BH for all subjects	Mean (%)	SD (%)
(End inspiration BH- before BH)/before BH	**-9**	**6**
(End inspiration BH- after BH)/after BH	**-11**	**6**
(End expiration BH- before BH)/before BH	**-5**	**8**
(End expiration BH- after BH)/after BH	**-7**	**8**

Normalized SCG energy in the 0 –20 Hz (p<0.05)

Change in the energy in the 0-20 Hz for all subjects	Mean (%)	SD(%)
(End inspiration BH- Normal breathing)/Normal breathing	**-10**	**11**
(End Expiration BH- Normal breathing)/Normal breathing	**-8**	**11**

HF (p<0.05)

Change in HF for all subjects	Mean (%)	SD (%)
(End inspiration BH- Normal)/Normal	**-58**	**27**
(End expiration BH- Normal)/Normal	**-78**	**12**

Conclusions and Future Work

- SCG Clusters are not completely separated based on respiratory flow rate or by lung volume.
- There was a reduction of SCG waveform variability by about 20% with clustering($p<0.05$) and 32% with breath holding ($p<0.05$).
- There was an 8% drop ($p<0.05$) in heart rate and a 68% drop ($p<0.05$) in heart rate energy in the 0.15-0.4 Hz range during BH cases.
- Normalized SCG energy was 9% lower ($p<0.05$) in breath holding than normal breathing.
- It may be useful to collect SCG during breath holding (since variability is lower).
- In future studies, other unsupervised machine learning algorithms will be used to cluster SCG events during regular breathing, and other supervised classifiers will be used to calculate the decision boundary.
- Future studies in a larger number of subjects are warranted to further verify these findings in healthy subjects and heart failure patients.

References

[1] B. S. Bozhenko, “Seismocardiography--a new method in the study of functional conditions of the heart,” Ter. Arkh., vol. 33, p. 55, 1961.

[2] D. M. Salerno, “Seismocardiography: A new technique for recording cardiac vibrations. concept, method, and initial observations,” J. Cardiovasc. Technol., vol. 9, no. 2, pp. 111–118, 1990.

[3] R. S. Crow, P. Hannan, D. Jacobs, L. Hedquist, and D. M. Salerno, “Relationship between seismocardiogram and echocardiogram for events in the cardiac cycle,” Am. J. Noninvasive Cardiol., vol. 8, pp. 39–46, 1994.

[4] K. Tavakolian, G. Portacio, N. Tamddondoust, G. Jahns, B. Ngai, G. Dumont, and A. Blaber, “Myocardial contractility: A seismocardiography approach,” in Engineering in Medicine and Biology Society (EMBC), 2012 Annual International Conference of the IEEE, 2012, pp. 3801–3804.

[5] A. Taebi, “Characterization, Classification, and Genesis of Seismocardiographic Signals,” Department of Mechanical and Aerospace Engineering, University of Central Florida, 2018.

[6] A. Taebi, R. H. Sandler, B. Kakavand, and H. A. Mansy, “Seismocardiographic Signal Timing with Myocardial Strain,” in Proceedings of the IEEE Signal Processing in Medicine and Biology Symposium (SPMB), 2017, pp. 1–2.

[7] S. Virani, A. Alonso, H. Aparicio, E. Benjamin, M. Bittencourt, C. Callaway, A. Carson et al., “Heart disease and stroke statistics—2021 update: a report from the American Heart Association,” Circulation, vol. 143, pp. e254–e743, 2021.

[8] T. Hassan, L. Mckinney, R. Sandler, A. Kassab, C. Price, F. Moslehy and H. Mansy, “An Acoustic Approach for Detection of Developmental Dysplasia of Hip,” in Proceedings of the IEEE Signal Processing in Medicine and Biology Symposium (SPMB), Philadelphia, PA, 2018, pp. 1-6.

[9] T. Hassan, “Detection of DDH in Infants and Children Using Audible Acoustics,” Department of Mechanical and Aerospace Engineering, University of Central Florida, Orlando, FL, 2019.

[10] T. Hassan, L. Mckinney, R. Sandler, A. Kassab, C. Price, F. Moslehy and H. Mansy, “A System for Measuring Sound Transmission Through Joints,” in Proceedings of the IEEE Signal Processing in Medicine and Biology Symposium (SPMB), Philadelphia, PA, USA, 2019, pp. 1-4.

[11] T. Hassan, R. Sandler, C. Price, A. Kassab and H. Mansy, “Detecting Hip Dysplasia Using Acoustic Excitation in a Pig Model,” in Proceedings of the IEEE Signal Processing in Medicine and Biology Symposium (SPMB), Philadelphia, PA, USA, 2020, pp. 1-3.

[12] J. Paparrizos and L. Gravano, “Fast and accurate time-series clustering,” ACM Trans. Database Syst., vol. 42, no. 2, p. 8, 2017.

[13] H. Sakoe and S. Chiba, “Dynamic programming algorithm optimization for spoken word recognition,” IEEE Transactions on Acoustics, Speech, and Signal Processing, vol. 26, pp. 43-49, 1978.

[14] D. F. Silva and G. E. Batista, “Speeding up all-pairwise dynamic time warping matrix calculation,” in Proceedings of the 2016 SIAM International Conference on Data Mining, 2016, pp. 837 845.

[15] J. Lei, “An extended BIRCH-based clustering algorithm for large time-series datasets,” Dissertation, Department of Information and Communication Systems, Mid Sweden University, SE, 2017.

[16] P. Gamage, M. Azad, A. Taebi, R. Sandler, and H. Mansy, “Clustering Seismocardiographic Events using Unsupervised Machine Learning,” in Proceedings of the IEEE Signal Processing in Medicine and Biology Symposium (SPMB), Philadelphia, PA, USA, 2018.

[17] R. H. Sandler, T. Hassan, B. Rahman, N. Raval, R. J. Mentz, and H. A. Mansy, “Seismocardiographic Signal Variability During Regular Breathing and Breath Holding,” Journal of Cardiac Failure, 2021.

[18] R. H. Sandler, T. Hassan, M. K. Azad, B. Rahman, N. Raval, R. J. Mentz, and H. A. Mansy, “Respiratory Phase Detection From Seismocardiographic Signals Using Machine Learning,” Journal of Cardiac Failure, 2021.

[19] C. Cortes and V. Vapnik, “Support-vector networks,” Machine Learning, vol. 20, no. 3, pp. 273-297, 1995.

UCF

Thank You

Questions?